Available online at www.sciencedirect.com

ScienceDirect

Procedia Engineering 81 (2014) 694 – 699

Procedia Engineering

www.elsevier.com/locate/procedia

11th International Conference on Technology of Plasticity, ICTP 2014, 19-24 October 2014, Nagoya Congress Center, Nagoya, Japan

Structural evolution of thin lamellar cementite during cold drawing of eutectoid steels

Gregory Gerstein[a], Florian Nürnberger[a,*], Włodzimierz Dudzinski[b], Dominika Grygier[b], Mirko Schaper[c], Andrzej Milenin[d]

[a]*Institut für Werkstoffkunde (Materials Science), Leibniz Universität Hanover, 30823 Garbsen, Germany*
[b]*Institute of Materials Science and Applied Mechanics, Wroclaw University of Technology, 50-370 Wroclaw, Poland*
[c]*Department of Materials Science, University of Paderborn, 33098 Paderborn, Germany*
[d]*AGH University of Science and Technology, 30-059 Kraków, Poland*

Abstract

Eutectoid steel wires are heat treated at isothermal temperatures to generate not only pearlitic microstructures but also bainite and martensite. These wires are subsequently drawn to increasing strain levels. The microstructural evolution is observed using scanning electron microscopy SEM and transmission electron microscopy TEM. Measurements of the lamellar spacing at different drawing stages reveal a thinning and a branching of the lamellae. In addition to this, the type of heat treatment influences the appearance of the lamellae and the formation of fine carbides. A numerical model was employed to compute the deformation conditions and the interlamellar spacing. The transformation and dissolution of cementite, branching of cementite and diffusion along dislocations were analysed with respect to various models from the scientific literature.

Selection and peer-review under responsibility of the Department of Materials Science and Engineering, Nagoya University

Keywords: Drawing; Pearlite; Lamellae; Branching

* Corresponding author: Tel.: +49 -511-762 4305; fax: +49 -511-762-5245.
E-mail address: nuernberger@iw.uni-hannover.de

1877-7058 © 2014 The Authors. Published by Elsevier Ltd. This is an open access article under the CC BY-NC-ND license
(http://creativecommons.org/licenses/by-nc-nd/3.0/).
Selection and peer-review under responsibility of the Department of Materials Science and Engineering, Nagoya University
doi:10.1016/j.proeng.2014.10.062

1. Introduction

Wire is employed in severely loaded components: such as steel rope, in cranes, elevators and as tyre cords. Owing to its good combination of strength and formability properties, pearlitic wire having a eutectoid composition is frequently employed. The fraction of cementite in pearlitic steels amounts to only 10 % to 20 % of the volume, however, this fraction mainly determines the mechanical properties. The strength of pearlitic steels is inversely proportional to the square root of the cementite lamellar spacing (Langford, 1977). Thus the plasticity of pearlitic wire will be increased with decreasing lamellar thickness. The carbon concentration in the ferritic matrix and the lamellar spacing can be specified by heat treating (Makarov et al., 2007).

1.1. Lamellae of pearlite and its change following deformation

Cementite lamellae can be characterised by their thickness, width and length (Sauvage et al., 2000). A measure of fineness of a lamellar structure is the true lamellar spacing, that is, the perpendicular distance between the two lamellae. The value of the apparent lamellar spacing varies between the colonies and depends on the angle at which the measuring plane intersects the lamellae. The intercept distance is measured along a line lying in a plane having an arbitrary direction which is not necessarily perpendicular to the lamellae. In order to determine the average intercept distance, several lines of a known length are projected on to the structure at different angles, and the total length of the lines are then divided by the number of intersected cementite lamellae (Ridley, 1984).

Electron micrographs show that the coarse and the fine pearlite structures behave differently during deformation (Porter et al., 1978). Pearlite which has fine lamellae exhibits larger plasticity than that in pearlite having coarse lamellae. It is assumed that the cementite lamellae in fine pearlite can sustain a larger plastic deformation as that in coarse pearlite (Langford, 1977; Gridnev et al., 1974; Porter et al., 1978). In coarse lamellar pearlite, comparatively coarse slip occurs in the ferrite whilst slip in the cementite takes place non-uniformly. In addition to this, entire pearlite colonies rotate during the deformation. The cementite lamellae can fracture which is assisted by the brittleness of the cementite lamellae (Porter et al., 1978). Rupturing leads to comparatively flat fracture surfaces.

In fine pearlite, the deformation occurs by means of relatively uniform slip in both the ferrite as well as in the cementite. In axially orientated pearlite, the cementite lamellae are so ductile that necking occurs. Considerable branchings of the lamellae accompany the deformation of pearlite colonies (Porter et al., 1978).

1.2. Motion in pearlite

The dislocation motion in coarse and in fine lamellar pearlite is also different. In coarse and in fine lamellar pearlite, a Pitsch-Petch and a Bagaryatski orientation relationship exists between the ferrite and the cementite, respectively. The phase boundaries between ferrite and cementite are on the (112) and the $(\bar{2}\bar{1}\bar{5})$ planes in the fine and coarse pearlite, respectively. However, in the latter, no dislocation glide can occur (Bagaryatskiy, 1959; Petch, 1953; Pitsch, 1978). This leads to cementite branchings only being observed in fine lamellar pearlite. An elevation in the free surface energy in the increasingly thinner cementite lamellae leads to a destabilisation of the cementite during the deformation (Sauvage et al., 2000). The phase boundary surface area increases and the lamellar spacing decreases. The dislocation density at the phase boundaries increases and promotes the decomposition of the cementite (Li et al., 2011). On reaching a specific level of deformation, no further decomposition of cementite is observed (Li et al., 2011).

2. Experimental method

2.1. Objective

In the following investigations, the influence of different heat treatment routines on the pearlite's lamellar structure is to be considered. On the other hand, the change in form of the cementite's lamellae, as a result of the progressive drawing deformation is to be characterised. The chemical composition of the wire material employed is given in Tab. 1.

Table 1. Chemical composition of pearlitic wire in mass percent.

	C	Mn	Si	P	S	Cr	B
Wire A and B	0.813	0.41	0.219	0.094	0.045	0.024	0.029

2.2. Experimental procedure

Prior to wire drawing, the two wires were austenitised, quenched and isothermally soaked in a salt heating bath. Tab. 2 gives the corresponding heat treatment parameters.

Table 2. Heat treatment parameters.

	Austenitising temperature [°C]	Soaking time (s)	Quenchant	Soaking temperature (°C)	Soaking time (s)
Wire A	850	900	salt	350	300
Wire A	850	900	salt	370	300
Wire A	850	900	salt	390	300
Wire A	850	900	salt	480	300
Wire B	850	900	lead	600	300

The form, thickness and the cementite lamellar spacing was electron microscopically (SEM and TEM) examined following specific drawing steps. Fig. 1 shows the drawing steps for wires A and B. The final drawing diameters obtained for wires A and B were 0.27 and 0.21 mm, respectively. In the following, the main focus of attention is on the lamellar structure of the smallest wire diameter.

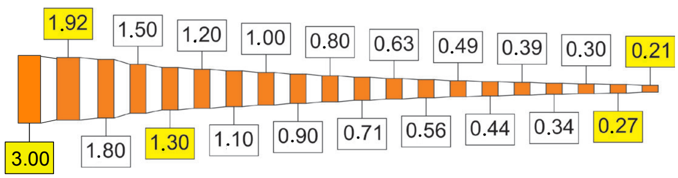

Fig. 1. Drawing steps for manufacturing thin wires for wire A (lower) and wire B (upper); the heat treatment according to Tab. 2 was performed for the drawing steps marked in yellow.

2.3. Numerical modelling

To numerically analyse the deformation of the multiphase pearlite colony, the following different initial dimensions of cementite lamellae and ferrite were used (Tab. 3). The details of the multi-scale FEM model employed were presented in Milenin et al. (2007, 2014).

Table 3. Variants of numerical simulations.

Variant	Thickness of cementite lamellae (nm)	Thickness of ferrite lamellae (nm)
a	40	15
b	20	15
c	40	8
d	20	8

To model the macro scale, a drawing pass was chosen having an initial wire diameter of 1.5 mm and a final diameter of 1.3 mm. A value of 0.03 was assumed for the friction coefficient. The micro scale was modelled along the deformation flow lines at distances of 1/4 of the wire's diameter measured from the wire's surface. The cementite's angle of inclination to the drawing direction at this position was assumed to be 28° based on the measurement of the lamellae mean gradient in the wire. The ratio of the mean stress to the loading stress of the respective phase was selected as the characteristic parameter with which the stress state of the cementite or ferrite can be estimated. Cumulative shear stress was selected as the parameter which characterises the deformed state.

3. Results

3.1. Heat treating and wire drawing

The TEM micrographs of wires A and B show the lamellar structure for wire diameters of 3.0 mm and 1.3 mm as well as the lamellar thicknesses and their spacings from each other (see Fig. 2). For a diameter of 3 mm, the cementite lamellae are uniformly arranged having a thickness of approx. 150 nm and a spacing of approx. 240 nm from each other. As a consequence of progressive deformation, the lamellae for a wire diameter of 1.3 mm are visibly thinner having a thickness of approx. 10 nm and spacings of approx. 30 nm from each other. In addition to this, branching lamellae and individual spherical carbides are visible. With the aid of SEM micrographs, Fig. 3 depicts the lamellar structure for the final wire diameters of wires A and B of 0.27 mm and 0.21 mm, respectively. As a consequence of the heat treatment, the microstructures differ despite the almost comparable level of deformation.

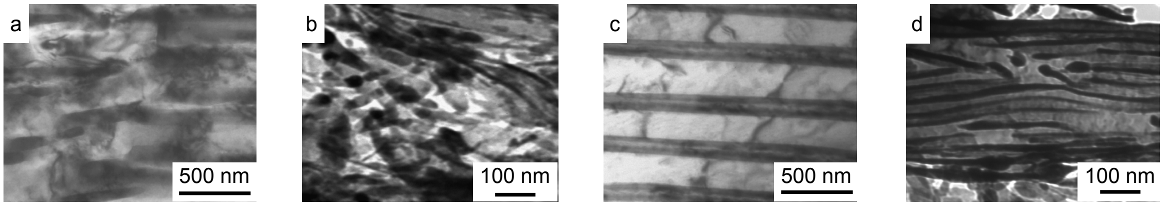

Fig. 2. Lamellar structure for wires A (a, b) and B (c, d) having diameters 3 mm (a ,c) and 1.3 mm (b, d).

Fig. 3 a and b, show that wire A's cementite lamellae have fragmented. The lamellae have markedly thinned and branched. Individual cementite particles are prominent at several locations. It can be seen from Fig. 3, c and d, that the lamellae in wire B are mainly unfragmented. They are essentially thicker than those in wire A and are markedly branched. There are almost no cementite particles visible which protrude from the lamellae. Individual, round cementite particles can be seen which have detached from the lamellae. Accordingly, the fragmentation of the lamellae, and thus the formability of the wire, depends on the heat treatment. Since the lamellae in wire B exhibit a larger thickness and lower fragmentation following drawing, these wires can be better drawn. The different heat treatments lead either to the formation of more orderly lamellae without fine carbide precipitates at the boundary between the cementite and ferrite matrix (Fig.3c and d), or to the formation of lamellae and spherulitic particles in the ferritic matrix (Fig.3a and b) (Schastlivtsev et al., 2002).

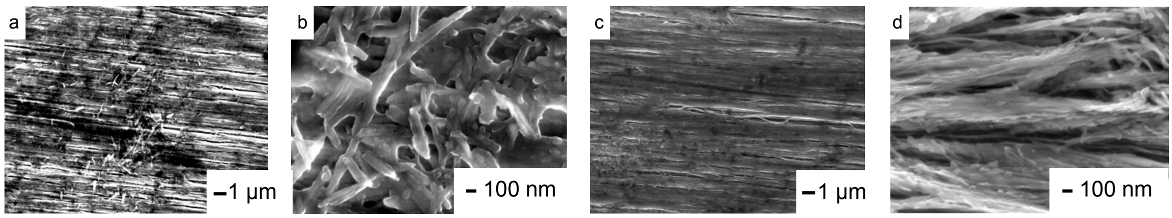

Fig. 3. SEM micrographs of wire A, diameter 0.27 mm (a, b) and wire B, diameter 0.21 mm (c, d) at different magnifications; in contrast to wire B, A shows very fine precipitates on the lamellar surfaces at high magnifications (deep etching using 2 % HNO_3, in-lens electron detector).

Using deep etching and by employing the in-lens detectors to depict the topology at high magnifications, it is possible to observe the lamellar branching. The branching of the cementite lamellae can be clearly recognised in Fig. 3d.

Tensile tests have been carried out to compare the mechanical properties of the wires, drawn after lead bath patenting at different temperatures. The temperature was varied between 320 °C and 600 °C. Subsequently, the wires were drawn to a cross-section diminution of 72.5 %. Wires treated at temperature less than 350 °C were not able to reach a cross-section diminution of 72.5 %. Comparing the wires treated with temperature between 370 °C and 480 °C no significant differences in the measured tensile strengths were observed. However, further steps of drawing revealed a higher plasticity by increasing the temperature. Only wires treated at temperature of 480 °C or higher, were able to reach a cross-section diminution of 97.8 %.

3.2. Numerical investigation

The results of the computed simulations show that:

- During the deformation, tensile stresses occur in the ferritic matrix and the cementite lamellae; the magnitude of the stress increases with decreasing lamellar thickness and decreasing lamellar spacing
- On reducing the lamellar spacing or the lamellar thickness, the level of shear deformation is slightly reduced in the cementite.

In this way, the tensile stress in the lamellae increases with decreasing lamellae thickness, but the magnitude of the shear deformation is lowered. The former reduces the ductility and the latter elevates the ductility. The tendency to disintegrate or branching the lamellae during the drawing process depends on the magnitude of each of these factors.

4. Discussion

4.1. Model of lamellar branching

The dissolution of fine phase fractions which, in this case, are represented as carbides, has been the object of various research activities for many years. Different theories exist for the decomposition of cementite in solidified microstructures. The extent to which carbides form, these can again dissociate due to various influences. One possible variation is the cutting of cementite lamellae by dislocation motion in which the carbon is dissociated from the carbide and accumulates around the dislocation. This effect is produced because the bonding enthalpy of the carbon to a dislocation in ferrite is greater than that to iron in cementite. Thus, the cementite is transformed into ferrite and interstitially dissolved carbon (Languillaume et al., 1997; Gridnev et al., 1982; Gavriljuk et al., 1985). Another theory claims that the interphasal boundary surface increases due to the plastic deformation. This can occur by means of the cementite lamellae becoming thinner as a consequence of their deformation and exhibiting phase boundaries having increased surface areas. In this case, the attempt of the thermodynamic system to minimise the free energy of the phase boundaries can be considered as the activator for the dissociation of the cementite (Nam et al., 2000; Hono et al., 2001; Languillaume et al., 1997).

The decomposition of the cementite differs for coarse and fine lamellar pearlite. In both cases, the fraction of cementite is lower for increasing strain. The lamellar spacing plays a very important role whilst the size of the colonies has no influence (Nam et al., 2000). In fine lamellar pearlite, the decomposition begins at a lower stress than that in coarse lamellae. It can be concluded from this that the cementite decomposition only then begins when the thickness of cementite lamellae has reduced below a definite size. The cementite's decomposition ceases as soon as the fraction of cementite sinks below a specific value. This can be attributed to a saturation of carbon in the dislocation at the cementite to ferrite boundary (Nam et al., 2000). According to Shin et al. (2000), the decomposition process of cementite occurs more quickly adjacent to dislocation structures. These lay on the cementite planes (101) and (103). The decomposition of the cementite leads to the formation of the characteristic layer formation and to partially dissolved lamellae. Thus, the facilitated outward flow of carbon into the ferrite leads to the formation of thin ferritic layers in the cementite lamellae and thereby to the branching (Shin et al., 2000). The longer the lamellar structure is maintained during the deformation, the more difficult their decomposition becomes. By continually decreasing the lamellar spacing, there is even less space for dislocations to pile up in the ferrite between the cementite lamellae (Izotov et al., 2008) and it is not possible for them to orientate themselves transverse to the lamellae. Thus, the piled-up dislocations lay longitudinal to the cementite lamellae direction and cannot cause cracks across the lamellae. Instead of this, they form longitudinal openings in the cementite lamellae which thereby become thinner and more branched. In coarse lamellar pearlite, the dislocations have sufficient space available between the lamellae to pile-up transversally and to fragment the lamellae. According to Y. Estrin und E. Rabkin (1998), edge dislocations play a more important role than screw dislocations for diffusion along dislocations. Since the wire is stretched during its drawing, deformation also occurs in this direction. For this reason, the dislocations' Burgers vector lies in the longitudinal direction and the dislocation line is perpendicular to it. Owing to the drawing process, the cementite lamellae also align themselves in the longitudinal direction and thereby lay perpendicular to the dislocation lines. The diffusion processes now occur along these lines. Thus, the carbon from the cementite lamellae can be directly transported into the adjacent ferritic layers.

5. Conclusion

The measurements of the lamellae spacings following various drawing passes have shown that the lamellae become finer and branching with increasing reductions in wire diameter. The type of heat treatment influenced the form and dimensions of the lamellae and the occurrence of fine carbides. A model was presented to illustrate lamellae branching as a result of drawing by taking into account dislocation movements. Further influences, such carbide formation due to heat treating, are to be investigated in continuing studies.

Acknowledgements

The authors would like to thank the German Science Foundation (DFG) for their financial support of the research work within the project SCHA 1484/16-1 and Armin Feldhoff for his support in the SEM measurements.

References

Bagaryatsky Y. A., 1950. The probable mechanism of decomposition of martensite, Doklady Akademii nauk SSSR. 73, 1161-1164.

Estrin Y., Rabkin E., 1998. Pipe Diffusion along curved dislocations: An Application to Mechanical alloying, Scripta Mater, 39(12), 1731-1736.

Gavriljuk V., Oskaderov S., 1985. Distribution of carbon in steel after a thermal-treatment and plastic deformation. Neue Hütte, 30, 361-366.

Gridnev V. N., Gavrilyuk V., Meshkov Y. Y., 1974. Strength and Plasticity of cold- deformed steel, Naukova Dumka, 231.

Gridnev V. N., Gavrilyuk V. G., 1982. Cementite decomposition in steel under plastic deformation. Phys Met+, 4 (3), 531-551.

Hono K., Ohnuma M., Murayama M., 2001. Cementite decomposition in heavily drawn pearlite steel wire. Scripta mater, 44(6), 977-983.

Izotov V. I., Pozdnyakov V. A., Luk´yanenko E. V., 2008. Evolution of the Dislocation Structure and the Formation of Fatigue Microcracks in Pearlitic-Ferritic Steels. The Physics of Metals and Metallography, 105(5), 517-527.

Langford G., 1977. Deformation of Pearlite, Metall Trans A, 8A(6), 861-875.

Languillaume J., Kapelski T., Baudelet B., 1997. Cementite dissolution in heavily cold drawn Pearitic steel wire. Acta Mater, 45(3), 1201-1212.

Li Y., Choi P., Borchers C., 2011. Atomic-scale mechanisms of deformation-induced cementite decomposition in pearlite. Acta Mater, 59(10), 3965-3977.

Makarov V., Savrai R. A., Schastlivtsev V. M., 2007. Mechanical properties and fracture upon static tension of the high-carbon steel with different types of pearlite structure. The Physics of Metals and Metallography, 104 (5), 522-543.

Milenin A., Kustra P., Byrska-Wojcik D., 2014. FEM-BEM code for the multiscale modeling and computer aided design of wire drawing technology for magnesium alloys. Adv Eng Mater,16 (2), 202-210.

Milenin A., Muskalski Z., Kustra P., 2007. PART 1 The multi-scale FEM simulation of wire fracture during drawing of perlitic steel. Mater Sci Forum, 575-578; 2008, PART 2, 1433-1438, 5th Int. Conf. ICPNS'07; Zhengzhou; China; 23.10 2007, Code 72567.

Nam W. J., Bae C. M., , Oh S. J. 2000. Effect of interlamellar spacing on cementite dissolution during wire drawing of pearlitic steel wires. Scripta mater, 42 (5), 457-463.

Petch N. J., 1953. The orientation relationships between cementite and -iron. Acta Crystallogr, 6(1), 96.

Pitsch W. D., 1963. Die kristallographischen Eigenschaften der Zementitaussscheidung im Austenit. Archiv für das Eisen, 34, 381-390.

Porter D., Easterling K., Smith G., 1978. Dynamic studies of tensile deformation and fracture of pearlite. Acta Metall Mater, 26,9,1205-1422.

N. Ridley, 1984. A Review of the Data on the Interlamellar Spacing of Pearlite, Metall Trans A, 15A(6), 1010-1036.

Sauvage X., Copreaux J., Danoix F., 2000. Atomic-scale observation and modelling of cementite dissolution in heavily deformed pearlitic steels. Philos Mag A, 80(4), 781-796.

Sauvage X., Guelton N., Blavette D., 2002. Microstructure evolutions during drawing of a pearlitic steel containing 0.7 at% copper. Scripta Mater, 46(6), 459-464.

Schastlivtsev V. M., Yakoleva I. L., Kar´kina L. E., 2002. Crystallographic Analysis of Defects in Cementite and Evolution of the Lamellar-Perlite Structure in Carbon Steel under Annealing. Doklady Physics, 47(6), 451-453.

Shin D., Kim B., Kim Y.-S., 2000. Microstructural evolution in a commercial low carbon steel by equal channel angular pressing. Acta Mater, 48(9), 2247-2255.